Biomarkers, November–December 2005; 10(6): 401–416

Taylor & Francis
Taylor & Francis Group

Characterization of the biochemical effects of 1-nitronaphthalene in rats using global metabolic profiling by NMR spectroscopy and pattern recognition

J. AZMI[1]*, J. CONNELLY[2], E. HOLMES[1], J. K. NICHOLSON[1], R. F. SHORE[3], & J. L. GRIFFIN[4]

[1]*Section of Biological Chemistry, Division of Biomedical Sciences, Imperial College of Science Technology & Medicine, London, UK,* [2]*Metabometrix Ltd., RSM, London, UK,* [3]*Centre for Ecology and Hydrology, Monks Wood, Abbots Ripton, Huntingdon, UK, and* [4]*Department of Biochemistry, University of Cambridge, Cambridge, UK*

Abstract

Metabolic fingerprints, in the form of patterns of high-concentration endogenous metabolites, of 1-nitronaphthalene (NN)-induced lung toxicity have been elucidated in bronchoalveolar lavage fluid (BALF), urine, blood plasma, and intact lung and liver tissue using NMR spectroscopy-based metabolic profiling. A single dose of NN (75 mg kg^{-1}) was administered orally to Sprague–Dawley rats. BALF and lung tissue were obtained 24 h after dosing from these animals and matched control rats post-mortem. High-resolution ^{1}H-NMR spectroscopy of BALF samples indicated that NN caused increases in concentrations of choline, amino acids (leucine, isoleucine and alanine) and lactate together with decreased concentrations of succinate, citrate, creatine, creatinine and glucose. In addition, the intact lung weights were higher in the NN-treated group ($p < 0.01$), consistent with pulmonary oedema. The NMR-detected perturbations indicated that NN induces a perturbation in energy metabolism in both lung and liver tissue, as well as surfactant production and osmolyte levels in the lungs. As well as reporting the first NMR spectroscopic combined examination of BALF and intact lung, this study indicates that such holistic approaches to investigating mechanisms of lung toxicity may be of value in evaluating disease progression or the effects of therapeutic intervention in pulmonary conditions such as surfactant disorders or asthma.

Keywords: *Metabonomics, metabolomics, biofluid NMR spectroscopy, pattern recognition*

(Received 28 March 2005; accepted 11 August 2005)

Introduction

1-Nitronaphthalene (NN) is a common environmental contaminant in airborne particulates in urban areas and is formed by nitration of polycyclic aromatic hydrocarbons (PAHs) during the combustion of diesel (Brorstrom-Lunden & Lindskog 1985, Draper 1986), and is a contributor to the mutagenic activity of

Correspondence: L. Griffin, Department of Biochemistry, University of Cambridge, Tennis Court Road, Cambridge CB2 1GA, UK. Tel: 44 (0)1223 333667. Fax: 44 (0)1223 766002. E-mail: jlg40@mole.bio.cam.ac.uk

*Present address: AstraZeneca R&D Charnwood, Development Drug Metabolism and Bioanalysis, Bakewell Road, Loughborough LE11 5RH, UK.

ISSN 1354-750X print/ISSN 1366-5804 online © 2005 Taylor & Francis
DOI: 10.1080/13547500500309259

airborne particles (Gupta et al. 1996). NN is also an intermediate in the production of a range of chemicals (Halladay et al. 1999). Both the lungs and the liver of rodents are damaged by exposure to NN, although the lung appears to be the more sensitive target. Single doses of NN given intraperitoneally (100 mg kg^{-1}; Johnson et al. 1984, Sauer et al. 1995) or orally (about 80–300 mg kg^{-1}; Verschoyle & Dinsdale 1990), produce a severe respiratory distress syndrome (RDS), chromodacryorrhea and bronchiolar epithelial injury.

NN-induced damage to rat lung proceeds through two morphologically distinct stages (Sauer et al. 1995, 1997). Swelling of the smooth endoplasmic reticulum and mitochondria of the non-ciliated epithelial (Clara) cells of the most distal bronchioles occurs within 1 h of exposure to NN. The second stage involves the infiltration of inflammatory cells into interstitial areas surrounding the damaged bronchioles and the onset of RDS, with this stage occurring some 4–6 h after treatment. This stage is also associated with progressive degeneration of the bronchiolar epithelium that involves both ciliated and Clara cells. Epithelial necrosis and exfoliation, marked interstitial oedema and pneumonitis remain evident 24 h after administration of NN. The formation of reactive metabolites of NN and/or reactive oxygen species in Clara cells appears to be responsible for the early damage to the bronchiolar epithelium, whereas later stage injuries can largely be ascribed to the marked inflammatory response (Sauer et al. 1995).

NN-induced hepatotoxicity manifests itself in the form of centrilobular and periportal hepatocellular necrosis, and bile duct epithelial necrosis (Johnson et al. 1984, Verschoyle & Dinsdale 1990). In intraperitoneal-dosed Sprague–Dawley rats, the injurious effects of NN on the liver have been observed to precede, and indeed may be responsible for, the lung damage. The changes accompanying liver toxicity include cytomegaly, loss of continuous inner membrane, and reduced matrix density of the mitochondria and mild multifocal necrosis. These changes are typically limited to a few hepatocytes in the centrilobular and periportal regions (Sauer et al. 1995, 1997).

The mechanism(s) of NN toxicity, its metabolism and biochemical sequelae have not been fully elucidated. The present study was designed to evaluate NN-induced changes in lung and liver function during the onset, progression and recovery of NN-dependent pulmonary and hepatotoxicity. High-resolution ^{1}H-NMR spectroscopy of rat urine, plasma and intact liver following a single oral dose (75 mg kg^{-1}) of NN provided metabolic profiles at specific time points in the progression of the lesion. The first high-resolution ^{1}H magic angle spinning (MAS)-NMR metabolic profiles of intact lung tissue and solution ^{1}H-NMR spectroscopy of BALF are also presented. The versatility of this technique is demonstrated by following the metabolic effects of NN-induced toxicity using a range of chemometric methods to interrogate the spectral profiles for evidence of metabolic perturbations.

Materials and methods

Animal handling and collection of biological samples

All work was carried out in accordance with procedures under the UK Animal (Scientific Procedures) Act 1986. There were two groups of rats. Group 1 was used in metabolism cage studies; group 2 consisted of satellite animals from which serial blood samples were taken. Both groups consisted of five NN-dosed and five control male Sprague–Dawley rats (Charles River, Margate, UK) that each weighed 290–340 g. All animals were housed under controlled environmental conditions (temperature 20°C, 55 ± 10%

relative humidity, 12 h light/12 h dark cycle) and provided with food (SQC Rat and Mouse Maintenance Diet No. 1, Special Diet Services, Witham, UK) and water *ad libitum*. The rats were acclimatized for 5 days in standard group rat laboratory cages and for 1 day in metabolism cages (group 1 only) before dosing. A single dose of NN (75 mg kg^{-1} body weight in 0.5 ml corn oil) or corn oil alone (control rats) was administered by oral gavage.

Rats in group 1 were housed individually in metabolism cages (five treated rats, five control rats). Urine samples from each rat were collected over ice with the addition of sodium azide (0.1% w/v solution) to the collection vessel to minimize bacterial contamination. The collection periods were: predose (24-h collection period), 0–8, 8–24, 24–32, 32–48, 48–72, 72–96, 96–120, 120–144, 144–168 h post-dose (p.d.). Blood from the tail vein of rats in group 2 (non-metabolism cage animals, five treated rats, five control rats) was collected into heparinized microcentrifuge tubes at predose, 6 and 24 h p.d., centrifuged at 13 000 rpm for 2 min and the plasma stored. All biofluid samples were frozen and maintained at $-20^{\circ}C$ before ^{1}H-NMR analysis. Animals were killed by cervical dislocation at 24 h p.d. (group 2) or 168 h p.d. (group 1) and approximately 20-mg samples of the liver (left lateral lobe) and lung (right lobe) were immediately excised and snap-frozen in liquid nitrogen for storage at $-80^{\circ}C$ until required for analysis. The remaining portion of the lung right lobe was fixed in 10% saline-buffered formalin, embedded in paraffin wax, sectioned (3–4 μm), stained with haematoxylin and eosin, and examined by light microscopy.

Clinical observation analysis

Daily body weights and total urine volume for the collection period were recorded for rats in group 1. Intact whole liver and lung weights were noted for all animals in both groups 1 and 2. Results are expressed as mean ± standard deviation; the means of the control and treated groups in each group were compared by Student's *t*-test test ($p < 0.05$ as level of significance).

BALF sample collection and preparation for ^{1}H-NMR analysis

BALF was collected from NN-treated and control rats at 24 h p.d. (group 2) and at 168 h p.d. (group 1) according to the method of Roth (1981). The trachea was isolated and cannulated with plastic tubing *in situ*. Isotonic NaCl solution (0.9% w/v; 4 ml) at room temperature was introduced gently into the cannula and immediately withdrawn, the process was repeated, and the recovered lavage fluid volumes from the two washes were combined. BALF samples were subsequently centrifuged at 600*g* for 10 min at 4°C to remove precipitates, frozen and maintained at $-20^{\circ}C$ before ^{1}H-NMR analysis. A quantity of BALF (500 μl) was pipetted into sample vials for NMR analysis together with 100 μl TSP (3-trimethylsilyl-1-[2,2,3,3-$^{2}H_4$] propionate; 1 mM; internal standard) in deuterium oxide (D_2O).

^{1}H-NMR spectroscopy of BALF, urine and blood plasma

NMR data were acquired on a Bruker DRX-600 spectrometer operating at 600.13 MHz for ^{1}H observation (Bruker Analytische Messtechnik GmbH, Rheinstetten, Germany). A flow-injection system was employed for urine and BALF delivery and analysis using a 4-mm outer diameter ^{1}H-^{13}C Z gradient probe. Samples containing only D_2O and

TSP were used as wash samples in between and during runs. A 5-mm selective inverse probe was used in the analysis of plasma samples. Single-pulse spectra were acquired using a solvent pre-saturation pulse sequence to suppress water resonances (relaxation delay: -90°-t_1-90°-t_m-acquire-FID, where t_1 is the first increment of the NOESY pulse sequence (3 μs) and t_m is a mixing time of 150 ms (Bruker Analytische). The number of acquisitions acquired was varied according to the biofluid examined (32 for urine, 128 for blood plasma and 256 for BALF). Other spectral acquisition conditions used were as follows. Free induction decays (FIDs) were collected into 48 (urine), 64 (plasma) or 32 k (BALF) data points, spectral width = 12 019.2 (urine) or 9000 (plasma and BALF) Hz, acquisition time = 2.04, 3.5 or 1.36 s for urine, blood plasma, BALF, respectively, total pulse recycle delay = 3.04, 5.6 or 3.37 s (for urine, plasma, BALF, respectively), one level of zero filling and temperature = 27°C. The FIDs were multiplied by an exponential weighting function equivalent to a line broadening of 0.3 Hz before Fourier transformation. The CPMG (Carr–Purcell–Meiboom–Gill; Braun et al. 1996) sequence was used with a total spin-spin relaxation delay of 96.4 ms to measure spin-echo ^{1}H-NMR spectra of plasma (no zero filling). The assignment of ^{1}H-NMR biofluid spectra was made with reference to published data (Nicholson et al. 1995, Lindon et al. 1999) and selected two-dimensional NMR experiments [gradient ^{1}H-^{1}H correlated spectroscopy (COSY) spectrum (Hurd 1990) and J-resolved (JRES) spectroscopy] (Braun et al. 1996).

^{1}H-MAS-NMR spectroscopic analysis of intact lung and liver tissue

Approximately 20 mg intact lung or liver tissue were washed in D_2O (acting as a frequency lock) to remove residual surface blood. Samples were placed in zirconia 4-mm diameter Bruker MAS rotors and analysed by ^{1}H-MAS-NMR spectroscopy on a Bruker DRX-400 (lung tissue) or DRX-600 (liver tissue) spectrometers operating at 400.13 or 600.13 MHz, respectively. MAS spin rates of 4000 or 5000 Hz for lung and liver tissue were used, respectively. In both cases, sample temperature was set to 27°C for the duration of the NMR experiment. Analysis was performed using the above one-dimensional pulse sequence with presaturation with 128 transients collected into 64 k data points using a spectral width of 8000 Hz, an acquisition time of 4.09 s and a total pulse recycle delay of 6.24 s. A line-broadening factor of 1 Hz was applied to all one-dimensional spectra acquired.

Analysis of NMR spectral data

All ^{1}H-NMR spectra were manually corrected for phase and base line distortions within XWINNMR (Bruker GmbH, Karlsruhe, Germany). Spectra were referenced to TSP (δ0.0) for urine samples, whereas plasma, intact liver and lung MAS-NMR spectra were referenced to the CH_3 group of lactate (δ1.33). The spectra were subsequently data-reduced into 256 spectral integral regions, corresponding to the chemical shift range of δ0.2–10.0, using AMIX (version 2.7.2; Bruker). The region δ4.5–6.0 was set to zero integral to remove the effects of variations in the presaturation of the water resonance in all NMR spectra, and in the case of urine to alleviate cross-relaxation effects in the urea signal via solvent exchanging protons. Integration across the remaining 245 spectral regions was performed automatically

(Anthony et al. 1994) and the total integrated intensity of each spectrum normalized, thereby compensating for the differences in overall solute concentration between biofluid and tissue samples.

The resulting data matrix was analysed by pattern recognition methods within SIMCA-P (version 8, UMETRICS AB, Umea, Sweden). In the case of urine spectra, the spectral integral regions 2.54, 2.58, 2.66, 2.70 and 2.74 were merged and weighted accordingly to take account of a pH-dependent shift in the citrate resonances occurring within the buffering range. Similarly, the 2-oxoglutarate (2-OG) integral regions 2.46 and 3.02 were merged and similarly weighted. Thus, citrate and 2-OG were represented by one spectral region each, thereby simplifying loadings.

The analyses of mean-centred data were conducted using principal components analysis (PCA) and partial least-squares discriminant analysis (PLS-DA) (Wold et al. 1998). In PLS-DA of NMR spectral data, the *X*-matrix comprises of the spectral integral regions as for PCA. To encode a class identity, a *Y*-matrix of dummy variables, comprising of a series of ones and zeros, describes the class membership of each observation in the training set. This vector is used in the supervised pattern recognition. Where complete separation was not possible, orthogonal signal correction (OSC) was also performed, which is a filtering method applied to enhance separation of the two classes of NMR spectral data. This method calculates components orthogonal to *Y*, which are then subtracted from spectral data matrix, thereby improving performance of subsequent analysis (Wold et al. 1998, Brindle et al. 2002).

Results

Clinical observations

During the study, the group of NN-treated rats demonstrated respiratory distress syndrome (RDS) and chromodacryorrhea within 24 h of exposure, and two rats were terminated at 24 h p.d. following severe RDS. However, no gross internal abnormalities were detected at post-mortem and there were no significant differences between NN dosed and control rats in their body weight, urine volume or total liver weight. However, the weight of the lungs was significantly greater in NN-treated than in control rats at both 24 and 168 h p.d. (at 24 h control $= 2.20 \pm 0.03$ g; treated $= 2.63 \pm 0.26$ g, $p < 0.01$ and at 168 h control $= 2.51 \pm 0.24$ g; treated $= 2.89 \pm 0.09$ g; $p < 0.01$ at 24 and $p < 0.05$ at 168 h).

Lung histopathology

NN-treated rats had mild and moderate multifocal degeneration and necrosis of the bronchiolar epithelium, affecting both ciliated and non-ciliated cells. The more markedly affected animals showed cellular sloughing and ulceration, and occasional acute inflammatory cell infiltration or haemorrhage, with acute inflammatory cell exudates in the bronchiolar lumen and inflammatory cell infiltration in the lung parenchyma.

Biochemical effect of NN exposure on urine

Although the urine ^{1}H-NMR spectra of NN-treated rats superficially appeared similar to those of control animals, PCA analysis readily separated the two groups

for all the time points examined, except predose, with separation across PCs 1 and 2 (Figure 1a, b). PCA also demonstrated a clear temporal progression for metabolite changes in both NN-treated and control groups, so in all subsequent analyses changes

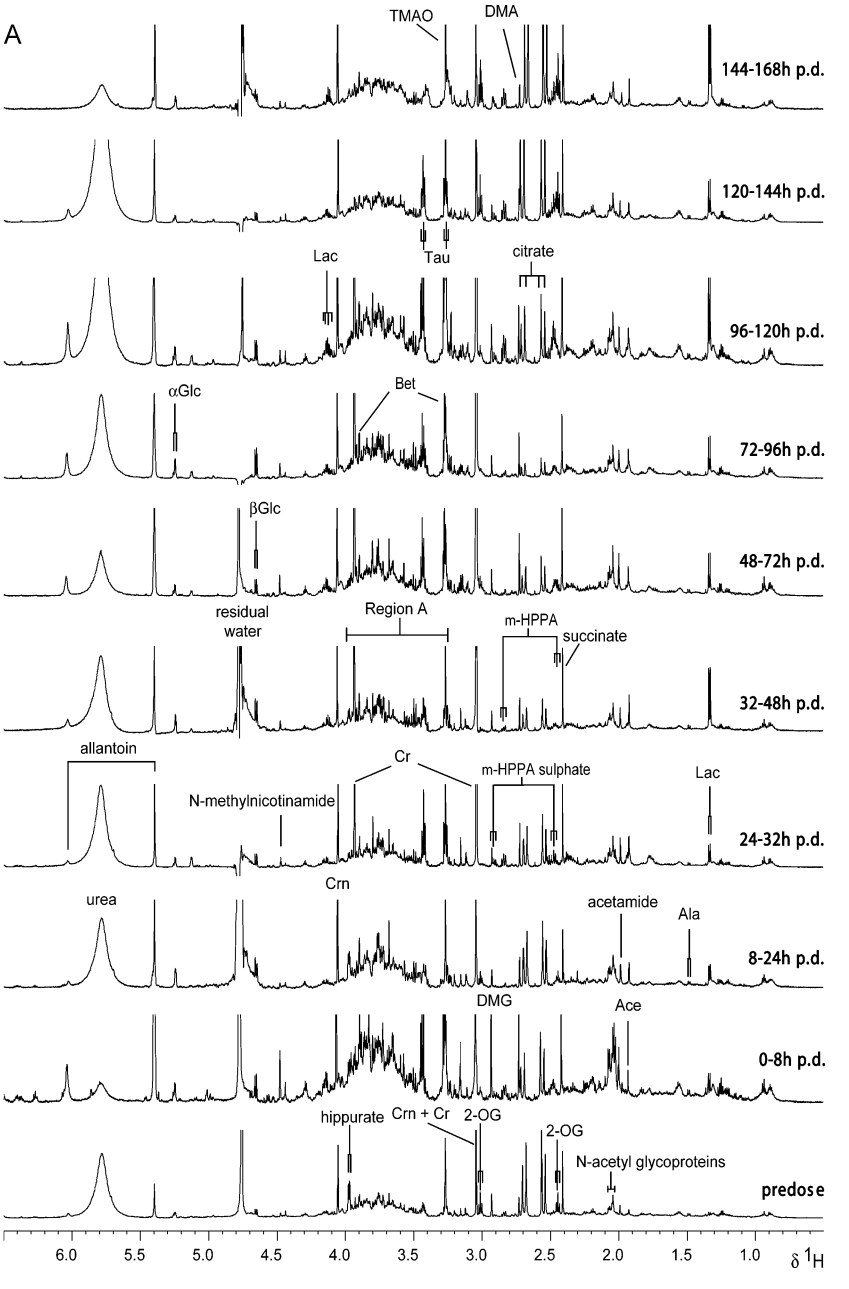

Figure 1. (A) 600-MHz ^{1}H single-pulse NMR spectra (δ0.5–6.5) of urine obtained predose and at various time points post-dose of 1-nitronaphthalene (75 mg kg^{-1}). Bet, betaine; ala, alanine; ace, acetate; 2-OG, 2-oxoglutarate; αGlc, α-glucose; βGlc, β-glucose; Cr, creatine; Crn, creatinine; DMA, dimethylamine; DMG, dimethylglycine; *m*-HPPA, *meta*-(hydroxyphenyl)propionic acid; TMAO, trimethylamine-oxide; lac lactate; tau, taurine; p.d., post-dose; region A, glucose and amino acid CH protons.

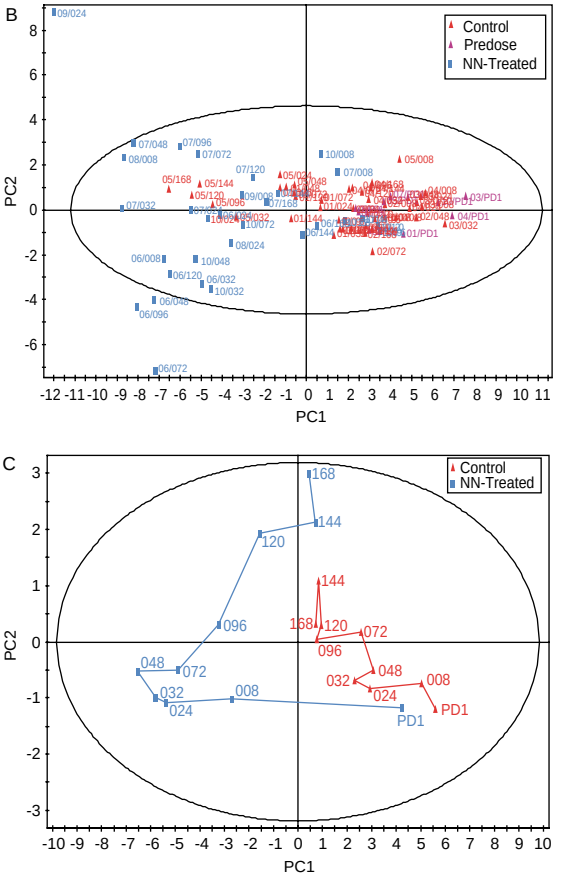

Figure 1 (Continued). (B) Plot of PCA scores of mean-centred spectra of urine from control rats and those dosed with 1-nitronaphthalene (75 mg kg^{-1}) treatment groups. Each data point is referenced by the first two digits referring to the animal number, and the last three digits referring to the urine collection time point. (C) PCA mean metabolic trajectory plot mapping the average position of urine NMR spectra for each time point. PCs 1 and 2 account for 49.9 and 75.6% of data variance in a and b, respectively. PD1, predose; 008, 0–8 h; 024, 8–24 h; etc.).

are referred to the control group at that time point, rather than being referenced to the predose group. The separation between the two groups was due to NN-treatment being associated with decreased excretion of citrate (0–120 h p.d.), 2-oxoglutarate (0–48 h p.d.), fumarate (0–96 h p.d.), hippurate (0–120 h p.d.), trimethylamine-*N*-oxide (TMAO) (8–120 h p.d.) and succinate (0–48 h p.d.), and increased concentrations of glucose (0–96 h p.d.), creatine (0–120 h p.d.), creatinine (8–96 h p.d.), acetate (8–120 h p.d.), lactate (0–144 h p.d.), betaine (24–120 h p.d.), taurine (24–48 h p.d.) and dimethylglycine (DMG) (0–72 h p.d.). At later time points, the levels of 2-oxoglutarate and succinate (72–120 h p.d.) were also higher in dosed than control animals.

NN-treated rats also demonstrated changes in a number of low concentration metabolites including increased concentrations of ketone bodies (0–8 h p.d.), acetamide (0–168 h p.d.), allantoin (0–144 h p.d.), *N*-methylnicotinamide (0–168 h p.d.), dimethylamine (DMA) (0–144 h p.d.), tyrosine (24–144 h p.d.), phenylalanine

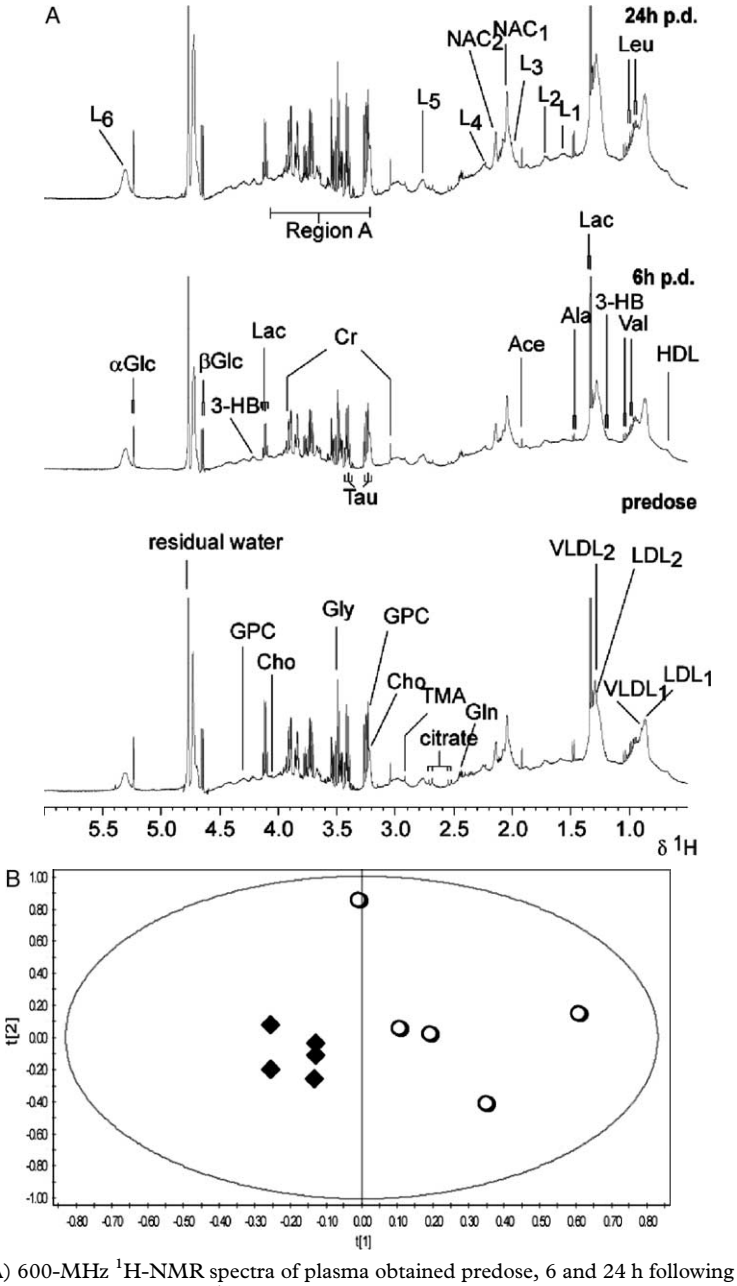

Figure 2. (A) 600-MHz ^{1}H-NMR spectra of plasma obtained predose, 6 and 24 h following administration of 1-nitronaphthalene (75 mg kg^{-1}). Key as for Figure 1 with the following additions: 3-HB, 3-D-hydroxybutyrate; Cho, choline; Gln, glutamine; Gly, glycine; GPC, glycerophosphocholine; HDL, C18 methyl from cholesterol in high-density lipoprotein; L_1, lipid CH_2*CH_2CO; L_2, lipid CH_2*$CH_2C=C$; L_3, lipid $CH_2C=C$; L_4, lipid CH_2CO; L_5, lipid $C=CCH_2$*$C=C$; L_6, lipid $C=CH$*CH_2CH_2; LDL_1, low-density lipoprotein terminal methyl; LDL_2, low-density lipoprotein $(CH_2)_n$; Leu, leucine; NAC_1/NAC_2, composite acetyl signals from α_1-acid glycoprotein; region A, glycerol, glucose and amino acid CH protons; TMA, trimethylamine; Val, valine; $VLDL_1$, very low density lipoprotein terminal methyl; $VLDL_2$, very low-density lipoprotein $(CH_2)_n$. (B) PCA scores plot of mean-centred plasma spectra collected at 24 h from control and 1-nitronaphthalene (NN, 75 mg kg^{-1}) treatment groups. PCs 2 and 3 account for 19.6% of the data variance. ○, Control; ◆ 24 h post-dose.

(8–32 h p.d.), phenylacetylglycine (PAG) (8–168 h p.d.), *meta*-(hydroxyphenyl) propionic acid (*m*-HPPA, 24–168 h p.d.), *m*-HPPA sulphate (96–168 h p.d.), and an unassigned chlorogenic acid metabolite (CAM, 96–168 h p.d.). Figure 1c shows the PCA analysis of the average NMR spectrum at each time point for the treatment and control groups, demonstrating the onset of toxicity as signified by a large displacement along PC1.

Biochemical effect of NN on blood plasma

Plasma from NN-treated rats was readily distinguishable from that from control animals at both 6 and 24 h p.d. This was due to increased concentrations of low-density lipoprotein (LDL) lipid, very low-density lipoprotein (VLDL) lipid, lactate, choline and glycerophosphochiline (GPC) in NN-treated rats (Figure 2a) and confirmed by PCA of the spectra from both time points (Figure 2b).

Biochemical effect of NN on BALF

The metabolic profiles from high-resolution ^{1}H-NMR analysis of BALF also readily distinguished NN-treated rats from controls using PCA, following OSC (Figure 3a, b). BALF collected 24 h p.d. from NN-treated animals had higher (compared with controls) concentrations of lactate, choline, leucine, isoleucine, alanine and N-acetyl groups of N-acetyl glycoproteins and lower levels of succinate, citrate, creatine, creatinine, glucose and hippurate as determined using the loadings plot of the post-OSC PCA model. BALF collected from NN-dosed animals 168 h p.d. had greater concentrations of lactate, acetate, N-acetyl groups of N-acetyl glycoproteins, succinate, creatine, choline, glycine, taurine, and *myo*-inositol than control BALF and lower concentrations of alanine, leucine and isoleucine. On inspection of the model, it was also found that OSC filtering before PCA resulted in the removal of uncorrelated variation corresponding to lactate in both control and treated spectra.

Biochemical effect of 1-NN on liver tissue

Although visual inspection failed to separate the liver tissue spectra for NN-treated rats from those for control animals, OSC and PCA or PLS-DA analysis did reveal differences (Figure 4), the OSC filter removing unrelated variation in the spectral regions corresponding to lipids, glucose and glycogen. Analysis of liver tissue collected 24 h p.d. showed NN-treatment caused increases in concentrations of lipids (largely triglycerides), choline, GPC, lactate, glucose, betaine, taurine and glycine, and a decrease in hepatic glycogen. At 168 h p.d., lipid, choline, GPC, lactate and glucose concentrations were still elevated in NN-treated animals but glycogen and alanine concentrations were also higher than in control liver. TMAO, taurine and betaine concentrations were reduced at 168 h p.d. compared with the control group.

Biochemical effect of NN on intact lung

Visual inspection again failed to distinguish biochemical differences between the lung tissue of NN-dosed and control rats (Figure 5a). However, following the exclusion of

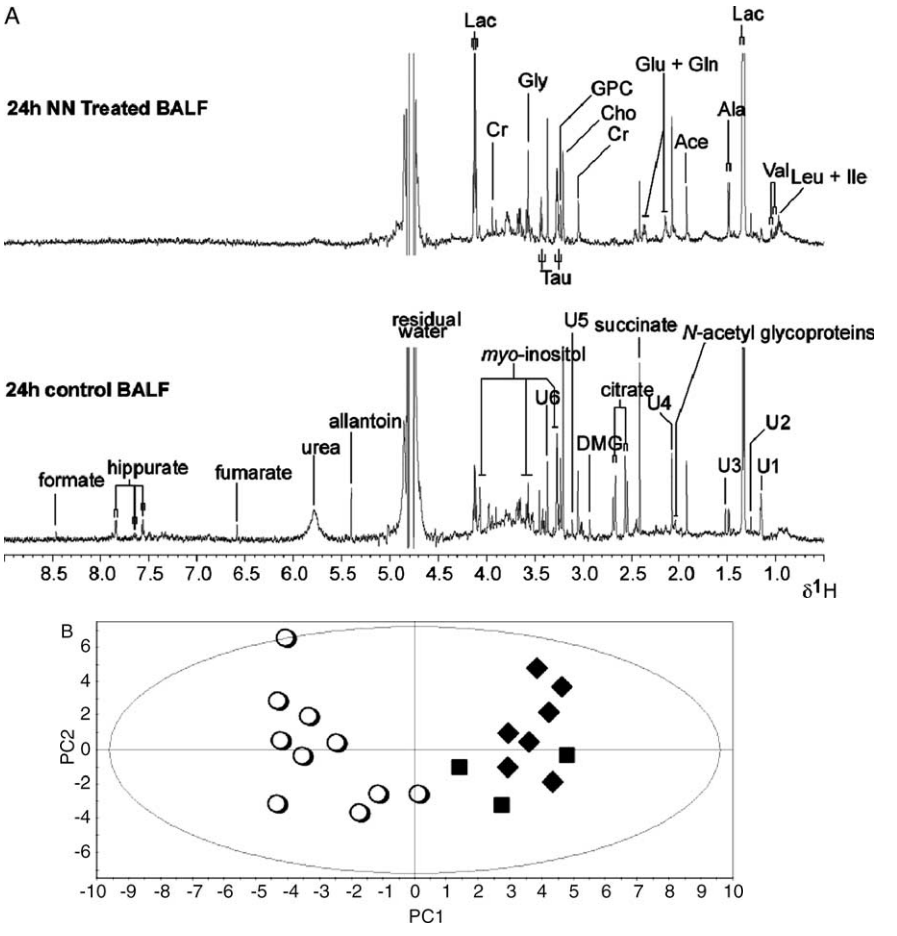

Figure 3. 600-MHz ^{1}H single-pulse NMR spectra (δ0.5–9) of BALF obtained from control and treated rats at 24 h following administration of 1-nitronaphthalene (NN, 75 mg kg^{-1}). Key is as for Figure 1 with the following additions: U1, U2, U3, U4, U5 and U6, unassigned singlets. (B) PCA scores plot of mean-centred OSC-filtered BALF spectra collected 24 and 168 h following treatment with 1-nitronaphthalene (NN, 75 mg kg^{-1}). PCs 1 and 2 account for 66.9% of the data variance. ○, Control; ◆ 24 h post-dose; ■, 168 h post-dose.

spectra from two rats in the control group due to abnormal lipid profiles, OSC filtering (which largely removed uncorrelated variation in the spectral integral regions corresponding to lipids and glucose) and subsequent PCA did separate the treatment and control groups (Figure 5b). At 24 h p.d., lung tissue from treated rats had more lipids and decreased concentrations of choline, GPC, taurine and glycine than tissue from control animals. The elevated lipid levels were still evident 168 h p.d. and were accompanied by increased concentrations of taurine, TMAO, choline, GPC, glycine and alanine.

Systemic effects of NN exposure

Table I shows the major fluctuations in metabolite profiles observed by ^{1}H-NMR spectroscopy over the time course in urine, plasma, liver, BALF and lung.

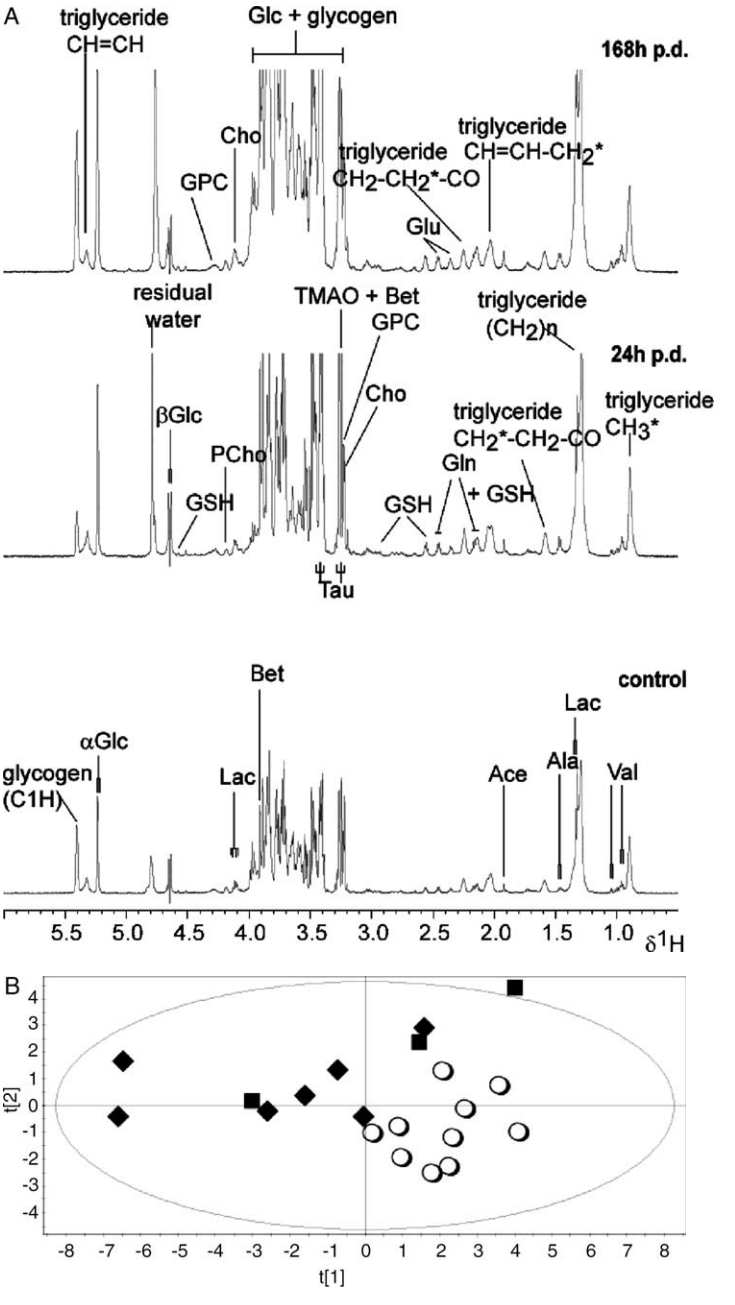

Figure 4. 600-MHz ^{1}H CPMG MAS NMR spectra of intact liver obtained 24 and 168 h post-dose of 1-nitronaphthalene (75 mg kg^{-1}). Key as for Figure 1 with the following additions: Glc, glucose; GSH, reduced glutathione. (B) Partial least-squares discriminate analysis scores plot of mean-centred CPMG intact liver obtained from control and 1-nitronaphthalene dosed (75 mg kg^{-1}) groups at 24 and 168 h following OSC spectral filtering. PLS-DA components 1 and 2 account for 76.9% of the data variance. ○, Control; ◆, 24 h post-dose; ■, 168 h post-dose. Two rats allocated to the 168-h group were terminated prematurely at 24 h post-dose due to severe respiratory distress syndrome.

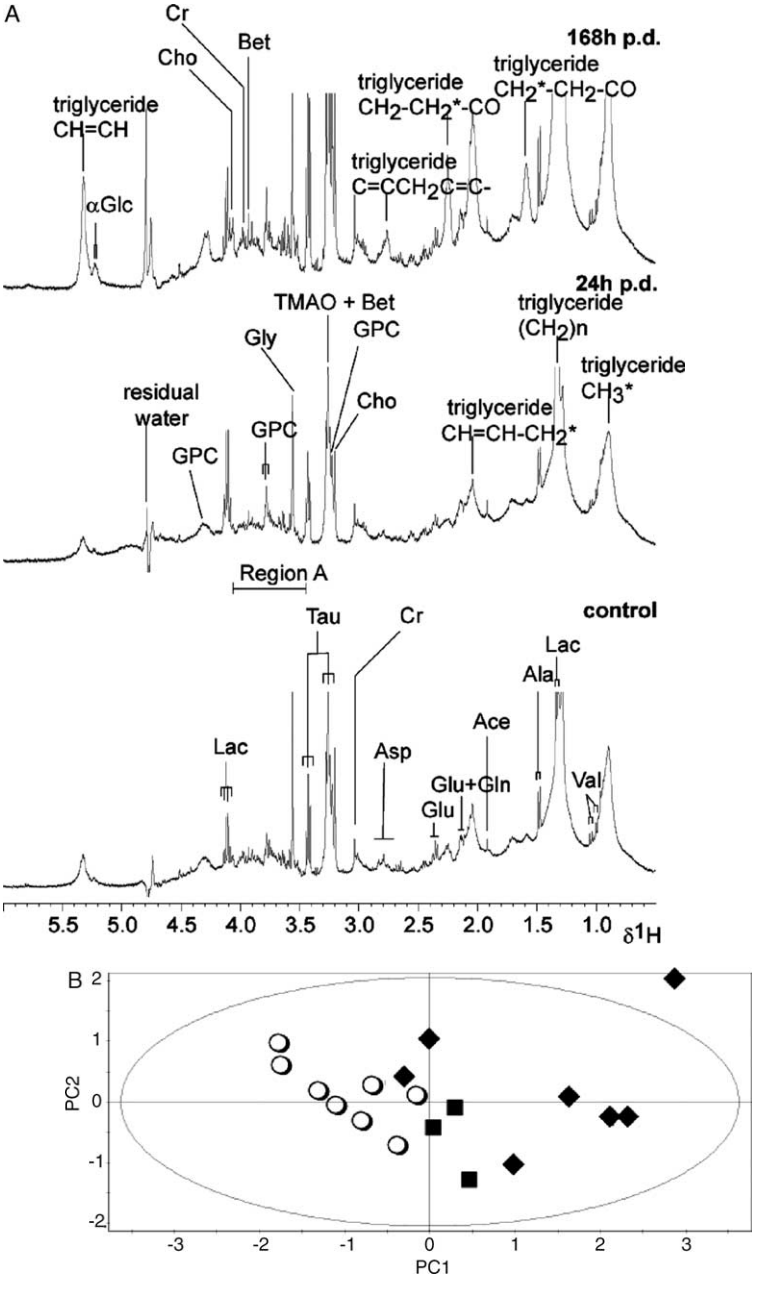

Figure 5. (A) 400-MHz ^{1}H-NMR spectra of intact lung from control animals and rats dosed with 1-nitronaphthalene (75 mg kg^{-1}) obtained at 24 and 168 h p.d. Key as for Figure 1. (B) PCA scores plot of mean-centred post-OSC data obtained from ^{1}H MAS-NMR spectra of lung collected 24 and 168 h post-dose compared with control animals. PCs 1 and 2 account for 80% of the data variance. ○, Control; ◆, 24 h post-dose; ■, 168 h post-dose.

Discussion

In this study, the metabolic effects of NN toxicity have been examined in both lung and liver tissues as well as in the biofluids urine, blood plasma and BALF. The aim was to cross-correlate metabolic changes in the intact tissues with those detected in the various biofluids so as to identify potential metabolic fingerprints associated with lung toxicity in these matrices.

Marked oedema in pulmonary tissue is a key feature of NN toxicity (Sauer et al. 1995), and is commonly accompanied by a significant increase in lung weight in NN-treated rats (Verschoyle & Dinsdale 1990, present study). However, the underlying mechanisms of NN-induced oedema remain uncertain. Previous studies of pulmonary oedema suggest the capillary wall may unload excess water (and proteins) into the airway space (King & Agre 1996). It is proposed that disruption of the bronchioles via NN-induced necrosis of bronchiolar epithelium is a contributing factor in oedema formation and the resultant pulmonary hypoxia. During the present

Table I. Summary chart illustrating the major fluctuations in metabolite profiles observed by ^{1}H-NMR spectroscopy in urine, plasma, liver, BALF and lung following 1-nitronaphthalene treatment (75 mg kg^{-1}).

Metabolite	Biomatrix studied, time point (h) and direction of deviation				
	Urine	Plasma	Liver	BALF	Lung
Citrate	↓0–168			↓24	
2-Oxoglutarate	↓0–168				
N-methylnicotinamide	↑0–168				
Ketone bodies	↑0–8				
Acetamide	↑0–168				
Allantoin	↑0–144				
Tyrosine	↑24–144				
Phenylalanine	↑8–32				
Succinate	↓0–120			↓24 ↑168	
PAG	↑8–168				
Lactate	↑0–168	↑6	↑24 ↑168	↑24 ↑168	
Acetate	↑8–168		↑168	↑168	
Alanine	↓8–72	↓6	↑168	↑24 ↓168	↑68
Leucine				↑24 ↓168	
Isoleucine				↑24 ↓168	
Glycine		↓6	↑24	↑168	↓24 ↑168
GSH			↑168		
Taurine	↑24–32		↑24 ↓168	↑168	↓24 ↑168
Creatine	↑0–120			↓24 ↑168	↑168
TMAO	↓8–96		↓168		↑168
Choline	↑8–96	↑6 ↑24	↑24 ↑168	↑24 ↑168	↓24 ↑168
GPC		↑6 ↑24	↑24 ↑168		↓24 ↑168
PCho			↑168		↓24
Glucose	↑0–120	↑6	↑24 ↑168	↓24	
Glycogen			↓24 ↑168		
Myo-inositol				↑168	↑24 ↑168
LDL/VLDL		↑6 ↑24			
Lipids		↑6 ↑24	↑24 ↑168		↑24 ↑168

GPC, glycerophosphocholine; GSH, glutathione; LDL, low-density lipoprotein; PAG, phenylacetylglycine; PCho, phosphocholine; TMAO, trimethylamine-*N*-oxide; VLDL, very low-density lipoprotein; ↑, above control levels; ↓, below control levels.

study, the concentration of several osmolytes in BALF increased at 168 h, including *myo*-inostol, choline, taurine and glycine, following an initial decrease at 24 h. This suggests that initial pulmonary oedema caused loss of lung tissue osmolytes before their longer-term production to maintain osmoregulation within the cells of the lung tissue.

NN-induced necrosis of the alveolar epithelium causes disruption of the surfactant-precursor containing cells, resulting in a reduction in lung surfactant and the well-documented sign of NN-induced lung toxicity, RDS (Sauer et al. 1995). *Myo*-inositol is a precursor of lung surfactant, and is normally present abundantly in mammalian cells (Jyonouchi et al. 1999). The NN-induced depletion of lung *myo*-inositol detected in BALF may either be a marker for decreased surfactant production or a depletion of cell numbers in pulmonary tissue in general. Holub (1986) reported that the abnormality in surfactant phospholipids in RDS is usually associated with low phosphatidylinositol and low plasma *myo*-inositol levels observed in a range of mammals, including humans. Alternatively, NN may act in a similar way to trichloroethylene, which decreases phospholipase A2 activity in mice. This enzyme controls the conversion of phosphatidylcholine to dipalmitoylphosphatidylcholine, the primary constituent of the lung surfactant (Scott et al. 1988). A perturbation in choline metabolism was detected in both liver and lung tissues, as well as increases in choline and GPC in blood plasma and BALF, which may reflect lowered surfactant production.

Failure to produce adequate concentrations of surfactants decreases the ability of oxygen to cross the alveolar lining, resulting in pulmonary hypoxia, as indicated in the present study by the increases in concentration of lactate and alanine in BALF. Pulmonary hypoxia would also increase epithelial cell necrosis and lysis, resulting in the release of many metabolites into BALF. Inflammation is known to increase membrane permeability in the lungs, and so many of the metabolites detected in BALF in the present study may be the result of increased permeability to constituents in blood plasma as well as due to the increased permeability of the lung cells themselves.

Many of the temporal biochemical changes detected in the urine and blood plasma are characteristic of generic toxic insults and have been detected in a number of renal and hepatic toxins (Beckwith-Hall et al. 1998). Indeed, many of these metabolic changes, in particular raised ketone bodies and a mobilization of lipids in blood plasma, as well as reduced TCA intermediates in urine, have been detected in rats during weight loss (Connor et al. 2004), and may relate to reduced food intake, before any animal weight loss. In addition, many of the urinary metabolites that were altered by NN toxicity, including PAG, *m*-HPPA and its derivatives, hippurate and chlorogenic acid, have been implicated as being derived from alterations in intestinal microbial populations (Nicholson et al. 2002, Nicholson & Wilson 2003). This suggests that either NN had a direct effect on the relative proportions of gut microflora or alterations in feeding had an impact on the metabolites produced by these microorganisms.

The present study has demonstrated that both NMR analysis of lung tissue and BALF can be used to monitor NN-induced pulmonary toxicity. While some of the metabolic changes detected in the lungs and BALF were reflected by changes in urine, blood plasma and liver tissue, the overall correlation between the two tissue types and three biofluids was poor, indicating different time courses and mechanisms of toxicity

across the animals. In the lung tissue, many of the metabolic changes reflected either increased permeability of pulmonary cells to metabolites in blood plasma, marked oedema or resultant hypoxia. Clinically, analysis of BALF may enable diagnosis and therapeutic monitoring of several lung diseases, such as asthma (Wright et al. 2000), surfactant disorders and other neonatal RDS conditions (Creuwels et al. 1997). It has gained popularity as a rapid *in vivo* screen to evaluate the toxicity of both systemic and inhaled pneumotoxins and is used in addition to the more classical methods to evaluate pathological changes (Day et al. 1990, Gupta et al. 1991). To date, alterations in specific biochemical and cytological constituents of BALF have been measured, but the present study has demonstrated how one can detect a number of NMR-detectable metabolites in BALF indiscriminately, and more importantly it has been illustrated how high-resolution ^{1}H-NMR spectroscopy and pattern recognition can be used to follow toxic insults in pulmonary tissue via the small metabolite changes in BALF and intact lung tissue.

Acknowledgements

British Gas Group Plc is acknowledged for its financial support to J. A. J. L. G. is a Royal Society University Research Fellow.

References

Anthony ML, Sweatman BC, Beddell CR, Lindon JC, Nicholson JK. 1994. Pattern recognition classification of the site of nephrotoxicity based on metabolic data derived from proton nuclear magnetic resonance spectra of urine. Molecular Pharmacology 46:199–211.

Beckwith-Hall BM, Nicholson JK, Nicholls AW, Foxall PJ, Lindon JC, Connor SC, Abdi M, Connelly J, Holmes E. 1998. Nuclear magnetic resonance spectroscopic and principal components analysis investigations into biochemical effects of three model hepatotoxins. Chemical Research in Toxicology 11:260–272.

Braun S, Kalinowski H-O, Berger S. 1996. 100 and More basic NMR experiments: a practical course. Weinheim: VCH.

Brindle JT, Antti H, Holmes Elaine, Tranter G, Nicholson JK, Bethell HWL, Clarke S, Schofield PM, McKilligin E, Mosedale DE, Grainger DJ. 2002. Rapid and non-invasive diagnosis of the presence and severity of coronary heart disease using ^{1}H-NMR-based metabonomics. Nature Medicine 8:1439–1444.

Brorstrom-Lunden E, Lindskog A. 1985. Characterization of organic compounds on airborne particles. Environment International 11:183–188.

Connor SC, Wu W, Sweatman BC, Manini J, Haselden JN, Crowther DJ, Waterfield CJ. 2004. Effects of feeding and body weight loss on the ^{1}H-NMR-based urine metabolic profiles of male Wistar Han rats: implications for biomarker discovery. Biomarkers 9:156–179.

Creuwels LAJM, Van Golde LMG, Haagsman HP. 1997. The pulmonary surfactant system: biochemical and clinical aspects. Lung 175:1–39.

Day BJ, Carlson GP, DeNicola DB. 1990. Gamma-glutamyltranspeptidase in rat bronchoalveolar lavage fluid as a probe of 4-ipomeanol and alpha-naphthylthiourea-induced pneumotoxicity. Journal of Pharmacological Methods 24:1–8.

Draper MW. 1986. Quantitation of nitro- and dinitro-polycyclic aromatic hydrocarbons in diesel exhaust particulate matter. Chemosphere 15:437–447.

Gupta GS, Kaw JL, Naqvi SH, Dixit, Ray PK. 1991. Inhalation toxicity of methyl isocyanate: biochemical and cytological profile of bronchoalveolar lavage fluid in rats. Journal of Applied Toxicology 11:157–160.

Gupta P, Harger W, Arey J. 1996. The contribution of nitro- and methylnitronaphthalenes to the vapor-phase mutagenicity of ambient air samples. Atmosphere and Environment 30:3157–3166.

Halladay JS, Sauer JM, Sipes IG. 1999. Metabolism and disposition of [^{14}C]1-nitronaphthalene in male Sprague–Dawley rats. Drug Metabolism and Disposition 27:1456–1465.

Holub BJ. 1986. Metabolism and function of myo-inositol and inositol phospholipids. Annual Reviews in Nutrition 6:563–597.

Hurd RE. 1990. Gradient-enhanced spectroscopy. Journal of Magnetic Resonance 87:422–428.

Johnson DE, Riley MGI, Cornish HH. 1984. Acute target organ toxicity of 1-nitronaphthalene in the rat. Journal of Applied Toxicology 4:253–257.

Jyonouchi H, Sun S, Iijima K, Wang M, Hecht SS. 1999. Effects of anti-7,8-dihydroxy-9,10-epoxy-7,8,9,10-tetrahydrobenzo[a]pyrene on human small airway epithelial cells and the protective effects of myo-inositol. Carcinogenesis 20:139–145.

King LS, Agre P. 1996. Pathophysiology of the aquaporin water channels. Annual Reviews in Physiology 58:619–648.

Lindon JC, Nicholson JK, Everett JR. 1999. NMR spectroscopy of biofluids. Annual Reports on NMR Spectroscopy 38:1–88.

Lindon JC, Nicholson JK, Holmes E, Everett JR. 2000. Metabonomics: metabolic processes studied by NMR spectroscopy of biofluids. Concepts in Magnetic Resonance 12:289–320.

Nicholson JK, Connelly J, Lindon JC, Holmes E. 2002. Metabonomics: a platform for studying drug toxicity and gene function. Nature Reviews in Drug Discovery 1:153–161.

Nicholson JK, Foxall PJD, Spraul M, Farrant RD, Lindon JC. 1995. 750 MHz ^{1}H and ^{1}H-^{13}C NMR spectroscopy of human blood plasma. Annals of Biochemistry 67:793–811.

Nicholson JK, Wilson ID. 2003. Opinion: understanding 'global' systems biology: metabonomics and the continuum of metabolism. Nature Reviews in Drug Discovery 2:668–676.

Roth RA. 1981. Effect of pneumotoxicants on lactate dehydrogenase activity in airways of rats. Toxicology and Applied Pharmacology 57:69–78.

Sauer JM, Eversole RR, Lehman CL, Johnson DE, Beuving LJ. 1997. An ultrastructural evaluation of acute 1-nitronaphthalene induced hepatic and pulmonary toxicity in the rat. Toxicology Letters 90:19–27.

Sauer JM, Hooser SB, Sipes IG. 1995. All-trans-retinol alteration of 1-nitronaphthalene-induced pulmonary and hepatic injury by modulation of associated inflammatory responses in the male Sprague–Dawley rat. Toxicology and Applied Pharmacology 133:139–149.

Scott JE, Forkert PG, Oulton M, Rasmussen MG, Temple S, Fraser MO, Whitfield S. 1988. Pulmonary toxicity of trichloroethylene: induction of changes in surfactant phospholipids and phospholipase A2 activity in the lung. Experimental Molecular Pathology 49:141–150.

Wold S, Antti H, Lindgren F, Ohman J. 1998. Orthogonal signal correction of near-infrared spectra. Chemometrics and Intelligent Laboratory Systems 44:175–185.

Wright SM, Hockey PM, Enhorning G, Strong P, Reid KBM, Holgate ST, Dukanovic R, Postle AD. 2000. Altered airway surfactant phospholipid composition and reduced lung function in asthma. Journal of Applied Physiology 89:1283–1292.